Understanding the active copper sites of Cu/ZrO$_2$ catalyst applied to direct conversion of ethanol to ethyl acetate and hydrogen

A. G. SATO[1,*]; D. P. VOLANTI[3]; J. V. NICÁCIO[1], E. LONGO[3]; J. M. C. BUENO[2].

[1]*Departamento de Química – Engenharia Química, Universidade Federal de Viçosa (UFV), Viçosa, 36570-000.*
[2]*Departamento de Engenharia Química, Universidade Federal de São Carlos (UFSCar), São Carlos, 13565-905*
[3]*Instituto de Química, Universidade Estadual Paulista (UNESP), Araraquara, 14800-900*
*E-mail para contato:agsato@ufv.br.

ABSTRACT – The origin and influence of active sites on supported copper catalysts, and their catalytic properties for ethanol conversion, were investigated using Cu/SiO$_2$, Cu$_2$O/SiO$_2$, and Cu/ZrO$_2$. Diffuse reflectance infrared Fourier transform spectroscopy of adsorbed CO revealed that Cu^{1+} was more prevalent than Cu^0 species at the Cu/SiO$_2$ surface, and that Cu^0 was the main species on Cu/ZrO$_2$. The Cu^{1+}/Cu^0 pair provided by Cu/SiO$_2$ generates sites that are highly selective for the dehydrogenation of ethanol. Ethyl acetate can be formed from ethanol and acetaldehyde at ZrO$_2$ or Cu surfaces. A combination of the Cu^{1+}/Cu^0 pair and Cu^0 interfaced to ZrO$_2$ is needed to efficiently transform ethanol to ethyl acetate.

1. Introduction

There is increased interest in ethanol chemistry as a way to increase the production of chemicals such as ethyl acetate, acetaldehyde, hydrogen, and others. The approach, based on green chemistry, employs renewable resources (Ruppert *et al.*, 2012). Copper-based catalysts have been successfully employed for the selective conversion of ethanol to ethyl acetate or acetaldehyde (Chang *et al.*, 2003; Volanti *et al.*, 2011). The best results for selective conversion of ethanol to ethyl acetate have been achieved with ZrO$_2$-supported copper catalysts (Iwasa and Takezawa, 1991; Inui *et al.*, 2002; Gaspar *et al.*, 2010; Wang *et al.*, 2010). In the case of the Cu/ZnO/Al$_2$O$_3$/ZrO$_2$ catalyst, the active site for the coupling of ethanol and aldehyde is at the mixed metal-oxides surface, not at the Cu metal surface (Inui *et al.*, 2004). In addition, the co-existence of Cu^0 and Cu^{1+} over Cu/ZrO$_2$ might provide a synergistic interaction for the conversion of ethanol to ethyl acetate (Wang *et al.*, 2010). Although the presence of a certain amount of Cu^{1+} species over a Cu/ZrO$_2$ catalyst can be important for improving the selectivity to ethyl acetate, the contribution of support oxide phases it is not clear. A full understanding of the properties of the active sites for conversion of ethanol to ethyl acetate is crucial for the development of a selective catalyst.

In this paper, we investigate the properties of Cu species in the Cu/ZrO$_2$ and Cu/SiO$_2$ catalysts, in order to understand the nature of the active sites that contribute to the special abilities of

Cu/ZrO$_2$ for ethanol conversion. The prepared catalysts were characterized by X-ray diffraction (XRD) and temperature-programmed reduction (TPR). In-situ X-ray absorption spectroscopy (XANES) measurements supported the proposition that there are changes in Cu speciation in different supports during TPR in H$_2$. Finally, diffuse reflectance infrared Fourier transform spectroscopy (DRIFTS) was used to confirm the metal-support interactions. The findings were supported by experimental results for CO adsorption on Cu-supported catalysts.

2. Experimental

Commercial grade monoclinic ZrO$_2$ (Saint-Gobain NorPro) and amorphous SiO$_2$ (AEROSIL 380, Degussa) were used as supports. Cu/ZrO$_2$ and Cu/SiO$_2$ samples were prepared by incipient wetness impregnation of the support with a solution of Cu(NO$_3$)$_2$.2.5H$_2$O (98%, Aldrich) in methanol. The solids were dried at 373 K overnight, and calcined at 673 K for 5 h under a flow of synthetic air. The theoretical amount of Cu was about 10 wt%. Cu supported on ZrO$_2$ and SiO$_2$ is hereafter referred to as Cu/ZrO$_2$ and Cu/SiO$_2$, respectively. In an attempt to evaluate the performance of the Cu^{1+} species in the ethanol reaction, SiO$_2$ was impregnated with Cu$_2$O (reagent grade, Aldrich), resulting in a Cu$_2$O/SiO$_2$ sample containing 10 wt% of copper.

Samples were characterized by ex-situ X-Ray Diffraction, Temperature-programmed reduction (TPR), in-situ XANES during TPR and by diffuse reflectance FT-IR (DRIFT). Activity and selectivity measurements of the ethanol reaction were carried out in a continuous-flow, tubular fixed-bed glass reactor (10 mm i.d.), over the temperature range 473–548 K, at atmospheric pressure. Samples were reduced in-situ in a flow of pure H$_2$. Detailed of the experiments setups can be viewed at reference (Sato *et al.*, 2012).

3. Results and Discussion

XRD patterns of the ZrO$_2$ support and calcined Cu/SiO$_2$, Cu/ZrO$_2$, and Cu$_2$O/SiO$_2$ samples are shown in Figure 1A. Intensive XRD pattern peaks were obtained for the Cu/SiO$_2$ sample at 35.5º and 38.7º, corresponding to a crystalline monoclinic CuO phase with a tenorite structure (JCPDS 48-1548). For the Cu/ZrO$_2$ sample, peaks at 24.2º, 28.2º, 31.4º, and 34.3º were attributed to a monoclinic ZrO$_2$ phase (JCPDS 37-1484). The peaks at 35.5º and 38.7º, corresponding to CuO, were also detected for the Cu/ZrO$_2$ sample. Peaks at 36.4º and 42.3º for the Cu$_2$O/SiO$_2$ sample were assigned to the Cu$_2$O cubic phase (JCPDS 05-0667). Figure 1B depicts the TPR-H$_2$ profiles for the Cu/ZrO$_2$, Cu/SiO$_2$, and Cu$_2$O/SiO$_2$ samples. Cu/ZrO$_2$ exhibited two peaks, at 400 and 480 K. TPR peaks below 450 K are related to the reduction of well-dispersed Cu oxide species, indicating a strong CuO-ZrO$_2$ interaction. The peak at 480 K could be assigned to the reduction of CuO due to weak interaction with the ZrO$_2$ surface or bulk CuO, as confirmed by the XRD analyses. Cu$_2$O/SiO$_2$ exhibited one peak between 625 and 725 K, indicating the reduction of Cu$_2$O crystals. The higher temperature of reduction for Cu$_2$O than CuO is expected from the higher apparent activation energy of 27.4 kcal/mol for Cu$_2$O, compared to a value of 14.5 kcal/mol for CuO (Kim *et al.*, 2003). The Cu/SiO$_2$ sample showed overlapping peaks at 500, 550, and 600 K. The species at around 500 K was assigned to bulk CuO, while the species reducible at higher temperatures were indicative of CuO-SiO$_2$ interaction.
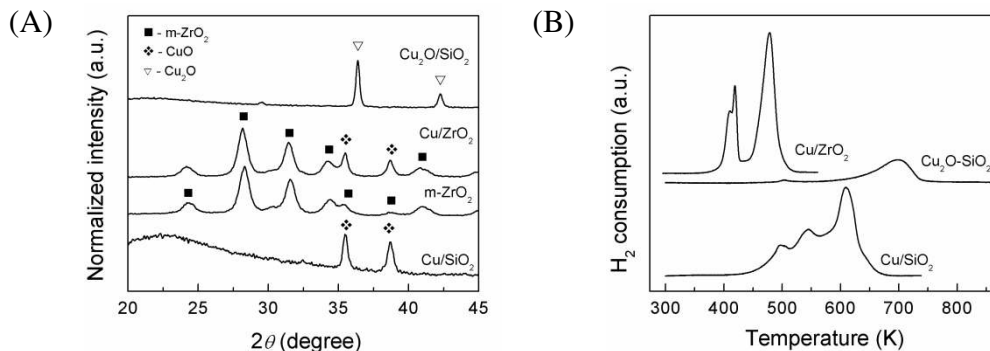
Figure 1. X-ray diffraction patterns for calcined Cu/SiO_2, ZrO_2 support, Cu/ZrO_2, and Cu_2O/SiO_2, (A). TPR-H_2 profiles for calcined Cu/SiO_2, Cu/ZrO_2, and Cu_2O/SiO_2 samples (B).

   Figures 2(A) and 2(B) present the evolution of the XANES spectra at the Cu K-edge, collected during TPR-H_2 experiments using Cu/SiO_2 and Cu/ZrO_2, respectively. The profiles of oxidation states of Cu as a function of temperature were obtained by applying a linear combination of spectra for the CuO, Cu_2O, and Cu foil standards. The reduction of copper oxide species supported on SiO_2 and ZrO_2 initiates at around 450 K. The content of Cu^{1+} species remains low in Cu/ZrO_2 catalysts, even when they are reduced at high temperatures. Although Cu/SiO_2 is totally reduced at high temperatures (up to 650 K, Figure 3C), a high amount of Cu^{1+} remained at temperatures at which the catalysts were reduced (500 K). The XANES results indicated that the reduction of CuO occurred in two steps ($Cu^{2+} \rightarrow Cu^{1+} \rightarrow Cu^0$). The equilibrium $Cu^{1+} \leftrightarrow Cu^0$ in small metallic Cu crystallites therefore depends on the standard free energy of formation, and hence on the morphology of the crystallite (Van Steen *et al.*, 2005). The oxidation of the metal is favored by a decrease in both metal particle size and temperature (Saib *et al.*, 2006; Knapp *et al.*, 2010).
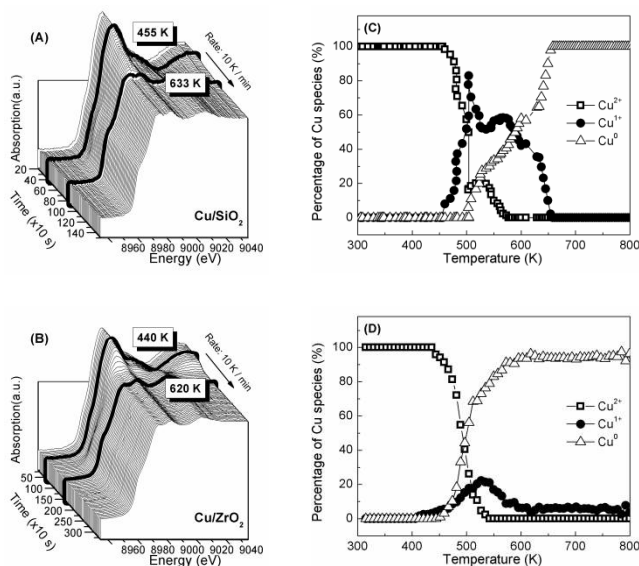

Figure 2. Time-resolved XANES spectra collected during TPR-H_2 for Cu/SiO_2 and Cu/ZrO_2 (A-B), and semi-quantitative evolution of copper species with increased temperature (C-D).

Adsorption of CO on Cu surfaces in different oxidation states has been shown to give rise to various species that exhibit IR absorption bands in the 2000–2200 cm^{-1} spectral region (Dandekar and Vannice, 1998). Figure 3 shows FT-IR spectra of CO adsorbed at 323 K on (A) Cu/SiO_2 and (B) Cu/ZrO_2 catalysts, where the IR band of adsorbed CO can be seen at 2125 and 2102 cm^{-1}, respectively. The observed shift in the IR band suggests the existence of significant structural and electronic differences between the Cu/SiO_2 and Cu/ZrO_2 samples. The adsorption of CO on Cu/SiO_2 produces the Cu^0-CO band at 2122 cm^{-1} in samples reduced at high temperatures (Hadjiivanov and Knozinger, 2001). On the other hand, Cu^0-CO species usually absorb at a lower frequency than that observed for Cu^{1+}-CO species. However, when copper is highly dispersed, Cu^0 forms carbonyls that can absorb at the same frequency as Cu^{1+}-CO carbonyls. In this case, the criterion of stability of the carbonyls has to be applied in order to distinguish Cu^0-CO from the Cu^{+1}-CO species (Milushev and Hadjiivanov, 2001). Higher stability characterizes a stronger σ-component of the Cu^{1+}-CO bond, and low stability characterizes a Cu^0-CO π-bond [19]. The spectra below the thicker lines in Figures 3(A) and 4(B) represents residual adsorbed CO after desorption at different temperatures for the Cu/SiO_2 and Cu/ZrO_2 catalysts, respectively. For the Cu/SiO_2 catalyst, a low thermal stability CO fraction was desorbed at 373 K, and another CO fraction was desorbed at a higher temperature (423 K). These results suggest that for Cu/SiO_2, the CO band at 2125 cm^{-1} corresponds to the overlap of Cu^0-CO and Cu^{1+}-CO species, which have low and high thermal stabilities, respectively. For the Cu/ZrO_2 catalyst, most of the adsorbed CO was of low thermal stability, suggesting that CO was mainly adsorbed on Cu^0 sites. The Cu^0-CO band for the Cu/SiO_2 and Cu/ZrO_2 catalysts was detected at 2125 and 2102 cm^{-1}, respectively. The shift of around 23 cm^{-1} in the IR band position, to a lower frequency, suggests stronger π back-donation from Cu^0 to CO, characterizing a higher electron density of Cu sites for the Cu/ZrO_2 catalyst than for the Cu/SiO_2 catalyst. Carbon monoxide can interact with either the Lewis acid $Zr^{δ+}$ cations or the Brønsted acid hydroxyl groups present at the surface of ZrO_2 (Jung and Bell, 2000).
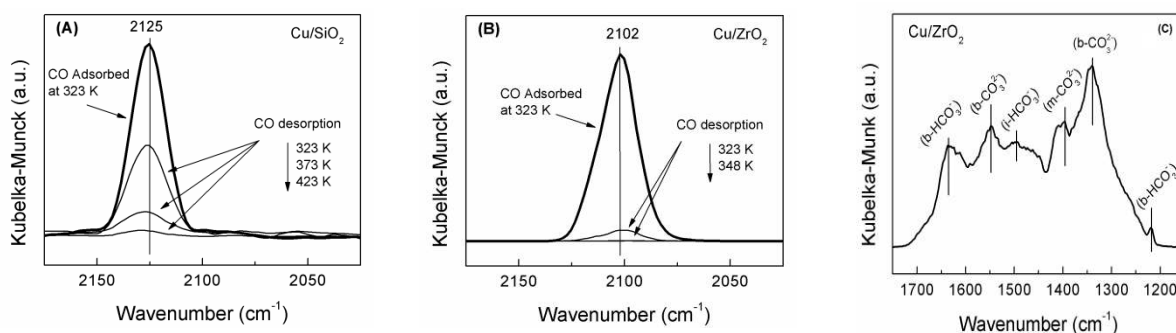

Figure 3. FT-IR spectra of adsorbed CO, and TPD, for (A) Cu/SiO_2 and (B) Cu/ZrO_2. Spectral region of copper. And at sectral region of zirconia (C). Thicker line: adsorption at 323 K.

The spectra of adsorbed CO in the ZrO_2 spectral region (1750 – 1150 cm^{-1}) are shown in Figure 3C for the Cu/ZrO_2 catalyst. Analogously to the interaction of CO_2 with ZrO_2, the formation of carbonate and bicarbonate species could be an indication of surface basicity associated with the presence of oxygen atoms (Hertl, 1989) and OH groups. The different surface species formed

upon CO adsorption can yield information on the existence of basic surface sites (basic hydroxyl groups and *cus* O^{2-} centers) or of acid-base pair sites (*cus* Zr^{4+}-O^{2-} centers) (Bianchi *et al.*, 1994). The CO adsorbed onto the Cu/ZrO$_2$ sample showed well-resolved bands at 1635, 1546, 1493, 1394, 1340, and 1218 cm^{-1}, related to the presence of different bonded CO species caused by the presence of basic centers and acid-base pair sites. The bands at 1635 and 1218 cm^{-1} were assigned to bidentate bicarbonates (b-HCO$_3^-$), whereas the bands at ca. 1546 and 1340 cm^{-1}, and at ca. 1394 cm^{-1}, were related to bidentate (b-CO$_3^{2-}$) and monodentate (m-CO$_3^{2-}$) carbonate species, respectively (Bianchi *et al.*, 1994; Pokrovski *et al.*, 2001). The band at 1493 cm^{-1} could be associated with the formation of ionic bicarbonate species (i-HCO$_3^-$). The bicarbonate species are usually formed by adsorption of CO onto basic hydroxyl groups. The formation of OH groups on the monoclinic ZrO$_2$ surface is assumed to be predominantly terminal (Bianchi *et al.*, 1994; Jung and Bell, 2000). Carbonate structures are formed via interaction of the oxygen in CO with Zr^{4+} cations in the lattice, as well as with a surface oxygen atom (Bianchi *et al.*, 1994; Jung and Bell, 2000). The bidentate carbonate surface complexes involve acid-base pair sites (*cus* Zr^{4+}-O^{2-} centers), while the monodentate carbonates involve strongly basic *cus* O^{2-} centers (Cerrato *et al.*, 1997; Bachiller-Baeza *et al.*, 1998; Cosimo *et al.*, 1998). The changes in catalytic activity and selectivity for ZrO$_2$, and for Cu supported on SiO$_2$ or ZrO$_2$, are shown in Table 1. The products formed during ethanol conversion on Cu/SiO$_2$ and Cu/ZrO$_2$ were ethyl acetate (AcOEt), acetaldehyde (AcH), methyl ethyl ketone (MEK), crotonaldehyde (CROT), propanone (PrO), CO, CO$_2$, ethylene (ETE), diethyl ether (DEE), and butanol (BOL). The action of Cu/SiO$_2$ was mainly in the dehydrogenation of ethanol, as shown by a selectivity for acetaldehyde (S_{AcH} = 87%). As has been reported previously (Duran, 2000), an increased loading of Cu on SiO$_2$ (not shown) resulted in increased selectivity for ethyl acetate, with the catalyst containing 35% of Cu loading (35Cu/SiO$_2$) showing a selectivity for ethyl acetate of S_{AcOEt} =45%.

The Cu$_2$O/SiO$_2$ catalyst was highly selective for dehydrogenation of ethanol to acetaldehyde (Table 1, run 7). Dehydrogenation activity on Cu$_2$O can be attributed to adsorption of ethanol to form CH$_3$CH$_2$O-Cu^{1+} species, and the ability of Cu^{1+}-O sites to undergo $^\beta$C-H scission to form acetaldehyde. Therefore, the high activity and selectivity for dehydrogenation of ethanol on Cu/SiO$_2$ was related to a predominance of Cu^{1+} sites. Unlike Cu/SiO$_2$, Cu/ZrO$_2$ showed high activity and selectivity for AcOEt, even at a low Cu loading. The Cu/SiO$_2$ and Cu/ZrO$_2$ catalysts showed activities and selectivities for ethyl acetate of r_{AcOEt} = 0.34 mmol/g$_{cat}$h, S_{AcOEt} = 5.3%, and r_{AcOEt} = 5.12 mmol/g$_{cat}$h, S_{AcOEt} = 73.0%, respectively. Nevertheless, Cu/SiO$_2$ and Cu/ZrO$_2$ showed similar selectivities for products of AcH condensation (such as MEK, BOL, and CROT). The products of ethanol dehydration were DEE and ETE. In an attempt to understand the nature of the active sites involved in formation of AcOEt, the ethanol was placed in contact with the ZrO$_2$ support. The results in Table 1 show that for ZrO$_2$ there was mainly dehydration of ethanol to DEE, while the activity for ethanol dehydrogenation was much lower for ZrO$_2$ than for Cu/ZrO$_2$. This finding is in agreement with DFT calculations (Chen and Ho, 2009), and indicates the low effectiveness of ZrO$_2$ for dehydrogenation of ethanol, due to a high barrier to $^\beta$C-H scission. As a result, adsorbed CH$_3$CH$_2$O-Zr(a) ethoxy species and stable species are formed on ZrO$_2$. Since ZrO$_2$ was unable to dehydrogenate ethanol, and was consequently not active for AcOEt involving AcH as a reactant, the ethanol was passed through a double bed reactor (two catalytic beds in series, separated with quartz wool), the first bed containing Cu/SiO$_2$, and the

second containing ZrO_2. Although the formation rate of AcOEt increased from r_{AcOEt} = 0.34 mmol/g_{cat}h, for Cu/SiO_2, to r_{AcOEt} = 0.70 mmol/g_{cat}h, for Cu/SiO_2//ZrO_2 (run 4), the formation rate was still lower than the r_{AcOEt} = 5.12 mmol/g_{cat}h obtained for the Cu/ZrO_2 catalyst. This result suggests that although AcOEt can be formed from ethanol and AcH on ZrO_2, the sites highly active for AcOEt are formed by the presence of Cu species on ZrO_2.

Table 1. Catalytic properties of Cu/ZrO_2, Cu/SiO_2 and Cu_2O/SiO_2 in ethanol dehydrogenation reaction from 473-523 K.

#	T (K)	Reactant Feed	Catalyst	Conversion (%)	Selectivity (%)						
					AcH	AcOET	MEK/BOL	CROT	DEE	ETE	Others**
1	498	EtOH	Cu/SiO_2	41	87	5.3	6.3	0.7	0.4	0.3	-
2	473	EtOH	Cu/ZrO_2	45	23	73	2.0	1.3	0.4	-	0.3
3	498	EtOH	ZrO_2	0.7	30	-	-	-	46	17	7.0
4	498	EtOH	(Cu//SiO_2 //ZrO_2)*	41	66	11	7.8	14	0.5	0.2	0.5
5	498	EtOH	Cu/SiO_2 + ZrO_2 mixed	47	51	11	18	19	0.6	0.1	0.3
6	473	EtOH + AcH	Cu/ZrO_2	43	32	54	5.3	7.4	0.2	0.1	1.0
7	523	EtOH	Cu_2O-SiO_2	15	100	-	-	-	-	-	-

EtOH: ethanol; AcH: Acetaldehyde; AcOET: ethyl acetate; MEK/BOL: methyl-ethyl-ketone and/or 2-butanol; CROT: crotonaldehyde; DEE: diethyl ether; ETE: ethylene. *(Cu//SiO_2 is separated and before of ZrO_2 bed. **Others (minor account): propanone, CO and CO_2.

Interestingly, comparison of runs 4 and 5 revealed that there was a higher selectivity for products of AcH condensation (CROT, MEK, and BOL) when the Cu/SiO_2 catalyst was physically mixed with ZrO_2. This suggests that intermediates of AcH formed due to the presence of Cu^{1+} species at the Cu^0 surface can be transferred onto the ZrO_2 surface by spillover, promoting formation of the condensation products of acetaldehyde . The results of runs 2, 3, and 4 showed that there was suppression of AcH condensation products (CROT, MEK, and BOL) when Cu was impregnated onto ZrO_2, suggesting that the Cu particles could have interacted with acid sites of the ZrO_2 surface, preventing the condensation by decreasing the density of acid sites. Reaction of ethanol on the ZrO_2 support formed products of the dehydration of ethanol (DEE and ETE). When ethanol and acetaldehyde in a ratio of 1.65 (EtOH:AcH) were passed over ZrO_2, the AcH condensation products (CROT, MEK, and BOL) were formed. This behavior suggests that strongly acidic sites were responsible for ethanol dehydration (Manríquez *et al.*, 2004), while dehydrogenation required moderately acid sites and strongly basic sites. On the other hand, acid sites can promote the β-aldolization reaction of acetaldehyde (Yee *et al.*, 2000). The DRIFTS analyses showed the presence of Cu^{1+} species with lower electron density over Cu/SiO_2, which should favor adsorption of ethoxy species, while for Cu/ZrO_2 the presence of a higher electron density Cu^0 species might favor the adsorption of acyl species. The results suggested that ethyl acetate formation occurred due to the combination of the Cu^{1+}/Cu^0 pair and Cu^0-ZrO_2 interface sites, which promoted the reaction between ethoxy species, mainly adsorbed over Cu^{1+} and $Zr^{\delta+}$ cations, and acyl species, mainly adsorbed over Cu^0. A detailed analysis of this effect will be the subject of a future paper.

4. Conclusion

In the Cu/SiO_2 catalyst, the Cu^{1+} species was more prevalent than Cu^0 at the surface and in the bulk material, in contrast to Cu/ZrO_2, where the main species was Cu^0. Accordingly, the Cu^{1+} provided by the Cu_2O/SiO_2 catalyst was highly selective for the dehydrogenation of ethanol, and the Cu^{1+}/Cu^0 pair provided by Cu/SiO_2 generated sites of very low selectivity for ethyl acetate and high selectivity for acetaldehyde. The efficient direct transformation of ethanol into ethyl acetate requires a combination of the Cu^{1+}/Cu^0 pair and high electron density Cu^0 chemically interfaced to ZrO_2.

5. Acknowledgements

6. References

BACHILLER-BAEZA, B.; RODRIGUEZ-RAMOS, I.; GUERRERO-RUIZ, A. Interaction of Carbon Dioxide with the Surface of Zirconia Polymorphs. **Langmuir,** v. 14, p. 3556-3564, 1998.

BIANCHI, D. et al. Intermediate species on zirconia supported methanol aerogel catalysts: III. Adsorption of carbon monoxide on copper containing solids. **Appl. Catal. A: Gen.,** v. 112, p. 57-73, 1994.

CERRATO, G. et al. A surface study of monoclinic zirconia (m-ZrO2). **Surf. Sci.,** v. 377-379, p. 50-55, 1997.

CHANG, F.-W.; KUO, W.-Y.; LEE, K.-C. Dehydrogenation of ethanol over copper catalysts on rice husk ash prepared by incipient wetness impregnation. **Appl. Catal. A: Gen.,** v. 246, n. 2, p. 253-264, 2003.

CHEN, Y.-W.; HO, J.-J. Dehydrogenation of Ethanol on a 2Ru/ZrO2(111) Surface: Density Functional Computations. **J. Phys. Chem. C,** v. 113, p. 6132 - 6139, 2009.

COSIMO, J. I. D. et al. Structure and Surface and Catalytic Properties of Mg-Al Basic Oxides. **J. Catal.,** v. 178, p. 499-510, 1998.

DANDEKAR, A.; VANNICE, M. A. Determination of the Dispersion and Surface Oxidation States of Supported Cu Catalysts. **J. Catal.,** v. 178, p. 621-639, 1998.

DURAN, R. M. **Thesis:** *Desidroacoplamento do etanol para acetato de etila sobre catalisadores de cobre suportados.* 2000. 135 (Doutorado). Departamento de Engenharia Química, Universidade Federal de São Carlos - UFSCar, São Carlos.

GASPAR, A. B. et al. The one-pot ethyl acetate syntheses: The role of the support in the oxidative and the dehydrogenative routes. **Appl. Catal. A: Gen.,** v. 380, p. 113-117, 2010.

HADJIIVANOV, K.; KNOZINGER, H. FTIR study of CO and NO adsorption and coadsorption on a Cu/SiO2 catalyst: Probing the oxidation state of copper. **Phys. Chem. Chem. Phys.,** v. 3, p. 1132-1137, 2001.

HERTL, W. Surface chemistry of zirconia polymorphs. **Langmuir,** v. 5, p. 96-100, 1989.

INUI, K.; KURABAYASHI, T.; SATO, S. Direct Synthesis of Ethyl Acetate from Ethanol Carried Out under Pressure. **J. Catal.,** v. 212, p. 207-215, 2002.

INUI, K. et al. Effective formation of ethyl acetate from ethanol over Cu-Zn-Zr-Al-O catalyst. **J. Mol. Catal. A: Chem.,** v. 216, p. 147-156, 2004.

IWASA, N.; TAKEZAWA, N. Reforming of Ethanol–Dehydrogenation to Ethyl Acetate and Steam Reforming to Acetic Acid over Copper-Based Catalysts. **Bull. Chem. Soc. Jpn.,** v. 64, p. 2619-2623, 1991.

JUNG, K. T.; BELL, A. T. The effects of synthesis and pretreatment conditions on the bulk structure and surface properties of zirconia. **J. Mol. Catal. A: Chem.,** v. 163, p. 27-42, 2000.

KIM, J. Y. et al. Reduction of CuO and Cu2O with H2: H Embedding and Kinetic Effects in the Formation of Suboxides. **J. Am. Chem. Soc.,** v. 125, n. 35, p. 10684-10692, 2003.

KNAPP, R. et al. Water-gas shift catalysts based on ionic liquid mediated supported Cu nanoparticles. **J. Catal.,** v. 276, p. 280-291, 2010.

MANRÍQUEZ, M. E. et al. Preparation of TiO2–ZrO2 mixed oxides with controlled acid–basic properties. **J. Mol. Catal. A: Gen.,** v. 220, p. 229-237, 2004.

MILUSHEV, A.; HADJIIVANOV, K. FTIR study of CO and NO adsorption and co-adsorption on Cu/silicalite-1. **Phys. Chem. Chem. Phys.,** v. 3, n. 23, p. 5337-5341, 2001.

POKROVSKI, K.; JUNG, K. T.; BELL, A. T. Investigation of CO and CO2 Adsorption on Tetragonal and Monoclinic Zirconia. **Langmuir,** v. 17, p. 4297-4303, 2001.

RUPPERT, A. M.; WEINBERG, K.; PALKOVITS, R. Hydrogenolysis Goes Bio: From Carbohydrates and Sugar Alcohols to Platform Chemicals. **Angew. Chem. Int. Ed.,** v. 51, n. 11, p. 2564-2601, 2012.

SAIB, A. M. et al. Preparation and characterisation of spherical Co/SiO2 model catalysts with well-defined nano-sized cobalt crystallites and a comparison of their stability against oxidation with water. **J. Catal.,** v. 239, n. 2, p. 326-339, 2006.

SATO, A. G. et al. Site-selective ethanol conversion over supported copper catalysts. **Catal. Commun.,** v. 26, p. 122-126, 2012.

VAN STEEN, E. et al. Stability of Nanocrystals: Thermodynamic Analysis of Oxidation and Re-reduction of Cobalt in Water/Hydrogen Mixtures. **J. Phys. Chem. B,** v. 109, n. 8, p. 3575-3577, 2005.

VOLANTI, D. P. et al. Insight into Cu-Based Catalysts: Microwave-Assisted Morphosynthesis, in Situ Reduction Studies and the Dehydrogenation of Ethanol. **ChemCatChem,** v. 3, p. 839-843, 2011.

WANG, L. et al. Direct transformation of ethanol to ethyl acetate on Cu/ZrO2 catalyst. **Reac. Kinet. Mech. Cat.,** v. 101, p. 365-375, 2010.

YEE, A.; MORRISON, S. J.; IDRISS, H. The reactions of ethanol over M/CeO$_2$ catalysts: Evidence of carbon-carbon bond dissociation at low temperatures over Rh/CeO$_2$. **Catal. Today,** v. 63, p. 327-335, 2000.